RESEARCH CENTER
"S.I.Vavilov State Optical Institute"

Institute for Physical Optics, Laser Optics and Information Optical Systems

Compact Autonomous Measuring System for Large Membrane Mirror

Final Report

Measuring system concept.
Experimental results

Contract F61775-99-WE038

Presented
for
European Office of Aerospace Research and Development
223/213 Old Marylebone Road, London, NW1 5TH,
United Kingdom

by
Adaptive Optical Systems Division

St.Petersburg
March,2000

REPORT DOCUMENTATION PAGE

Form Approved OMB No. 0704-0188

1. AGENCY USE ONLY (Leave blank)	2. REPORT DATE	3. REPORT TYPE AND DATES COVERED
	March 2000	Final Report

4. TITLE AND SUBTITLE

Compact Autonomous Measuring System For Large Membrane Mirror

5. FUNDING NUMBERS

F61775-99-WE038

6. AUTHOR(S)

Dr. Vadim A. Parfenov

7. PERFORMING ORGANIZATION NAME(S) AND ADDRESS(ES)

Institute of Physical Optics,
12, Birzhevaya liniya,
St. Petersburg, 199034
Russia

8. PERFORMING ORGANIZATION REPORT NUMBER

N/A

9. SPONSORING/MONITORING AGENCY NAME(S) AND ADDRESS(ES)

EOARD
PSC 802 BOX 14
FPO 09499-0200

10. SPONSORING/MONITORING AGENCY REPORT NUMBER

SPC 99-4038

11. SUPPLEMENTARY NOTES

12a. DISTRIBUTION/AVAILABILITY STATEMENT

Approved for public release; distribution is unlimited.

12b. DISTRIBUTION CODE

A

13. ABSTRACT (Maximum 200 words)

This report results from a contract tasking Institute of Physical Optics, as follows: The contractor will develop the concept and preliminary design of a compact autonomous measuring system that provides a display of the adaptive mirror figure and the error signal to a control system.

14. SUBJECT TERMS

EOARD, Space optics, Control System, Adaptive Optics

15. NUMBER OF PAGES

31

16. PRICE CODE

N/A

17. SECURITY CLASSIFICATION OF REPORT	18. SECURITY CLASSIFICATION OF THIS PAGE	19, SECURITY CLASSIFICATION OF ABSTRACT	20. LIMITATION OF ABSTRACT
UNCLASSIFIED	UNCLASSIFIED	UNCLASSIFIED	UL

NSN 7540-01-280-5500

Standard Form 298 (Rev. 2-89)
Prescribed by ANSI Std. 239-18
298-102

Table of contents

Page

Abstract 3

1. Introduction 4

2. Liquid-crystal Hartmann wavefront sensor 5

2.1. Controllable liquid-crystal hole array.....5

2.2. Principal optical configuration of the wavefront sensor.....7

2.3. Comments on methodology.....9

2.4. Calibration.....10

3. Two-wavelength dynamic holographic interferometry.....14

3.1. Measuring diffraction efficiency of the optically addressed liquid-crystal spatial light modulators.....14

3.2. Practical suggestions.....19

4. Preliminary comparison of LC Hartmann sensor and two-wavelength dynamic interferometer.....22

5.Membrane mirror for further investigations.....23

6. Summary table of considered methods.....27

7. Summary and conclusions.....29

8. References.....31

ABSTRACT

Principal and functional schematics of a liquid-crystal (LC) Hartmann wavefront sensor and two-wavelength dynamic holographic interferometer capable of measuring severe aberrations up to 2000 μm are proposed.

The LC Hartmann sensor can be implemented in different versions including Shack LC lenslet array, large focusing LC tunable lens or LC hole array. The simplest controllable LC hole array was manufactured and is under calibration at the moment.

The two-wavelength holographic interferometer allows one to test large aberrations in visible range with the help of conventional detector arrays as an interference pattern to be analyzed is formed at an equivalent wavelength much more than the wavelength of the radiation of the initial beams used. The main issue is a recording medium possessing high spatial resolution up to 1000 mm^{-1}. An optical set up for measuring the diffraction efficiency of holographic media, in particular, liquid-crystal spatial light modulators, was assembled. The investigations are in progress now. A preliminary comparison of both methods under investigations is given on the basis of the most important criteria (dynamic range, simplicity, possibility of real-time operation etc.). It is pointed out that additional experiments are needed using a 212 mm membrane mirror manufactured in the scope of the study.

A summary table of the considered method is presented including the main advantages and drawbacks of the method.

Practical comments and recommendations on the implementation of the devices developed and some proposals on the follow-on of the work are given.

1. Introduction

The current study is intended for searching the optimum method and developing a compact device (system) for measuring deformations of large membrane mirrors of 10...20 m in diameter. The dynamic range of measurements was estimated to be 1...2000 μm. Such unusual requirements determines the complexity of the task. A concept of the measuring system is expected to be developed and experimentally checked.

As was defined at the very beginning of the work (see the Phase 1 report, p.6), four regimes of measurements should be realized starting with the deployment of the mirror through accurate alignment and to surface maintaining:

a) coarse measurements during the initial deployment (hundreds and thousands of waves in visible range);
b) accurate measurements during the fine adjustment (from 1 to 100 waves);
c) high accuracy measurements during the surface maintenance (less than 1 wave);
d) emergency regime, i.e. repetition of regimes a), b), c) in the case of unforeseen breakage in the telescope.

We are trying to develop a system to cover all the mentioned regimes. But at the same time, it would be highly desirable to avoid any unreasonable complication of the system. Therefore, we do not exclude conducting the measurements in two stages, that implies using two and more devices simultaneously or consequently.

The results of our analysis and preliminary experiments at Phases 1 and 2 of the work have led us to the conclusion that three methods are worth comprehensive consideration and experimental investigations in the scope of the study:

- LC Hartmann method;
- two-wavelength dynamic holographic interferometry;
- wavefront curvature sensing by Roddier.

This report presents the main results of the theoretical and experimental work at the LC Hartmann wavefront sensor and two-wavelength dynamic interferometer capable of testing severe aberrations and covering huge dynamic range of tenths of wave to thousands waves. Also, a summary table of all the considered methods is given.

2. Liquid-crystal Hartmann wavefront sensor

Hartmann method was pushed up after our comparative analysis of different methods of wavefront measurements potentially capable of testing severe aberrations. Conventional Hartmann (or Hartmann-Shack) devices are featured by simplicity, reliability and nearly interferometric accuracy. Unfortunately, they are unable to measure huge local wavefront tilts because of the problem of "beam crossing". Our comprehensive consideration of contemporary technologies has led us to three concepts briefly described in Phase 2 report. They are based on using electrically controlled LC hole or lenslet arrays. The holes (lenslets) are turned on consequently, one by one. Such an operational mode allows us to avoid the "beam crossing" problem and dramatically increase the dynamic range of measurements. By the moment, we have this device manufactured. It is in the process of calibration and experimental investigations. The main drawback of the device is the sequential principle of scanning. It is probably acceptable if real-time operation is not highly necessary.

When our study was in progress, we got to know that a French group (Thomson-CSF) was also pursuing a LC Hartmann scanner concept [1]. Their concept is analogous to our simplest idea: a Hartmann hole array (screen) and a focusing lens behind it. This idea is under realization in our laboratory, and we expect to reach the maximum dynamic range for the sensor. In January 2000, we were informed that a group from AFRL had developed a LC Hartmann sensor and investigated it. We hope our results and practical recommendations will be helpful for the customer.

2.1. Controllable liquid-crystal hole array

The authors of [1] used a wavefront scanner based on a liquid-crystal television between two polarizers. It had 640×480 pixels, with a pixel pitch of 40 μm and a fill factor of ~0.56. The total surface of scanning was 25.6 by 19.2 mm. The pixels were grouped to define the sampling subapertures of 200 μm to 1mm.

We manufactured much simpler device shown schematically in Fig.2.1.

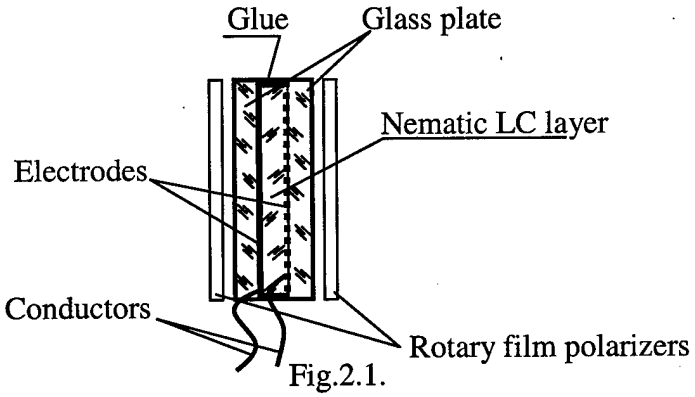

Fig.2.1.

A LC cell has two glass plates with 24 electrodes on each. The electrodes are transparent conducting strips of 1 mm width, the gaps between the electrodes are as small as 5...10 μm. The space between the plates is filled with nematic LC layer of 10 μm. Pulse voltage (potential) can be applied to all of the electrodes on both plates, but of different polarity. The LC cell is placed between two rotary film polarizers. The polarizers are mutually rotated until the transmittance of the whole system is minimum (the maximum voltage is applied to all electrodes). This ensures the maximum contrast of light intensity modulation. The dependence of the transmittance on the voltage between the electrodes is presented in Fig.2.2.

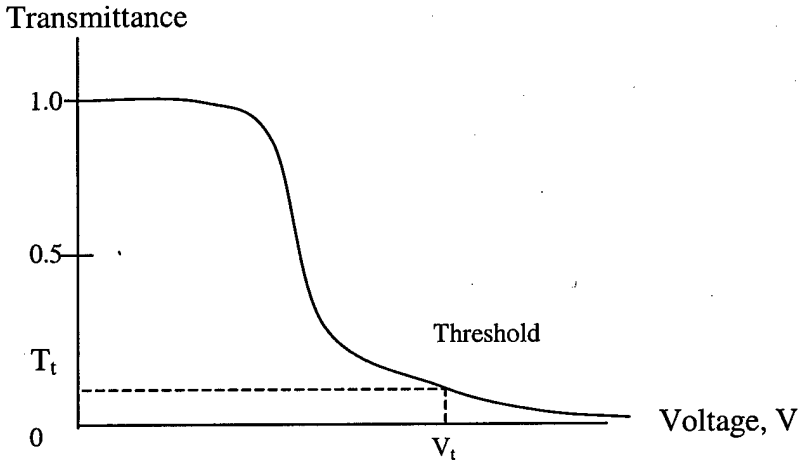

Fig.2.2.

When the voltage is maximum (pulses of opposite polarity on the electrodes) the transmittance is low, i.e. below the threshold T_t of the sensitivity of a defector. If the potential on one of the electrodes is zero, the voltage between the electrodes along the corresponding line or column is still larger than V_t and the transmittance is also below T_t. To open (turn on) a subaperture one should minimize (zero) the potential on the desired electrode (one more column or line). In this case, the voltage between the electrodes within the 1x1mm zone of their crossing is less than V_t, and the transmittance is maximum (close to 1.0).

The lens behind the output polarizers focuses pencil beams in the plane of the analysis (detector).

2.2. Principal optical configuration of the wavefront sensor

A principal (and functional) configuration of the LC Hartmann wavefront sensor is given in Fig.2.3 . The beam from the light source is focused near the center of curvature of the mirror under test (or focus of the holographic structure on the mirror) and illuminates the mirror after reflection from the beamsplitter. The retro-reflected beams partially passes the beamsplitter and are collected by the projection lens. The projection lens images the mirror surface near the LC hole array. Each subaperture of the LC hole array isolates a small 1x1 mm zone of the wavefront to be analyzed. The subapertures are turned on in desired order with the help of the controller. The lens behind the second polarizer focuses pencil beams on a CCD camera. A frame grabber is used to catch focal spot images to be analyzed. We use a Spiricon beam analyzer system LBA-300PC including Cohu-4915 CCD camera , frame grabber and a special software. The system measures and memorizes the positions of the spot centroids to be used to calculate the local tilts of the wavefront (angular aberrations) :

$$\frac{\partial W}{\partial x} \approx \frac{x'}{f'}$$

where W is the wave aberration, x' is the lateral displacement of the spot across the detector, f' is the focal length of the lens. The procedure of the measurements is followed by reconstructing the wavefront. The estimation can be of modal or zonal type, depending on the mirror surface control concept. The dynamic range of measurements for the central zone of the wavefront is determined by

$$\Delta\varphi = \frac{D}{f'},$$

where D is the CCD size.

The sensitivity (resolution) is estimated as

$$\delta\varphi = p/f',$$

where p is the CCD pixel size. If the minimum measurable spot displacement is m times less than the pixel size, then the sensitivity is m times better. There is a trade-off between dynamic range and sensitivity. The dynamic range is of our prime interest at the moment.

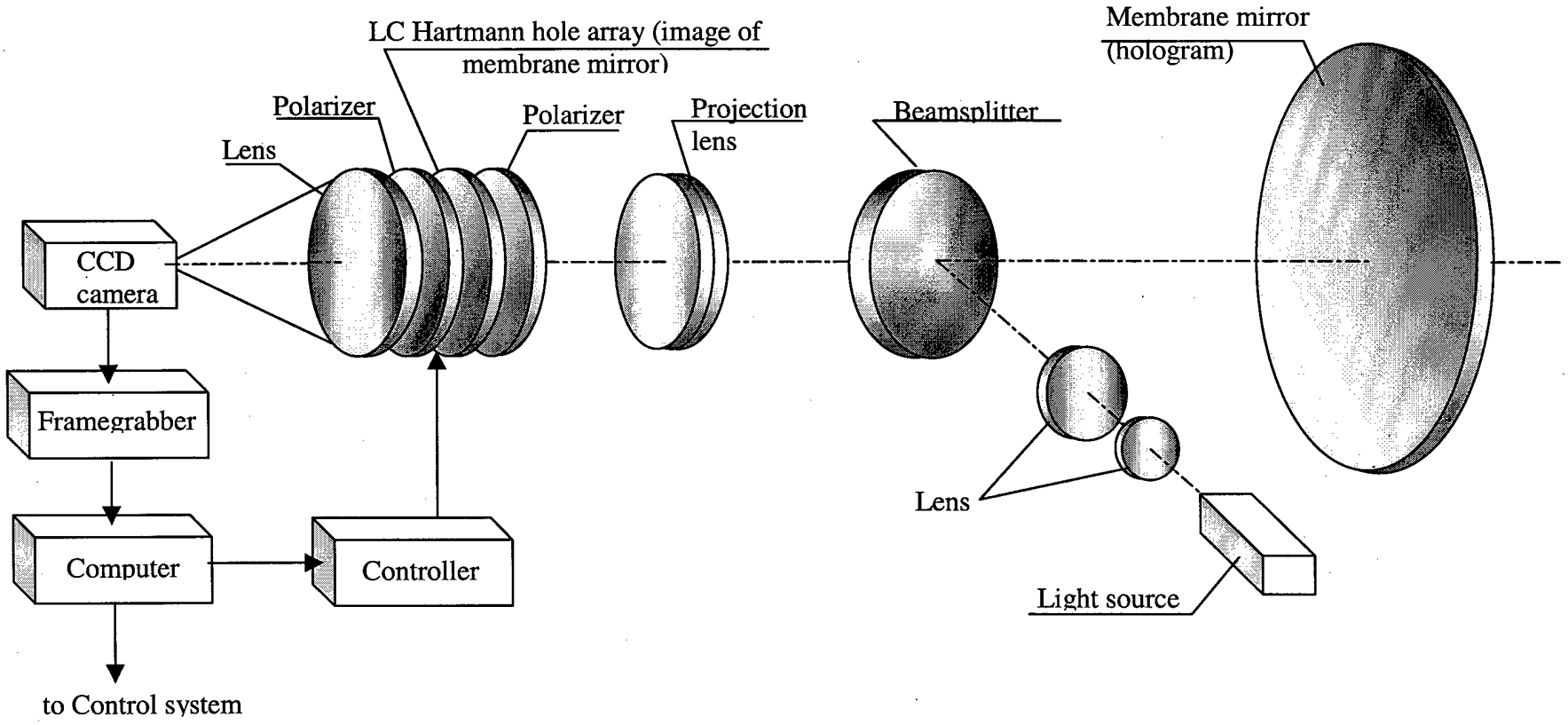

Fig. 2.3. Principal schematic of LC-Hartmann wavefront sensor.

2.3. Comments on methodology

There are some problems concerned with the processes of illuminating the mirror, re-imaging the mirror surface and focusing the beams from the Hartmann subapertures. We have practical comments on these questions to share.

Illuminating

The measurements of the mirror surface can be conducted either at the curvature center of the mirror or its focus. Of course, some initial alignment and focusing is needed according to a special techniques that are not considered within the current study. The mirror should be illuminated from its center of curvature, infinity (natural or artificial beacons, scene) or focus of the hologram structure on the mirror. As our estimates show, no continuous hologram is required. It can be fragmented, for example, consisting of many spots of 200...250 mm in diameter and with a fill factor of 1 and down to 0.5.

As the mirror is expected to be aspheric, a null lens will be most probably required for testing from the curvature center. It should be noted that null lenses operate in a limited range of the aberrations to be measured. A significant undercompensation is quite possible because the beams do not pass the appropriate zones of the null lens in reverse path. In the worst cases, the retro-reflected beams fail to enter the null lens.

We are trying to develop a wavefront sensor without null lenses to simplify it as much as possible. We anticipate the dynamic range of the wavefront sensor will be slightly decreased as test beams do not fall onto the mirror surface along the normals to it. Also, the algorithm of the data processing will be more complicated. Therefore, our experiments are intended for revealing possible systematic errors and potential limitations of the method. As was agreed on with the customer, the measurements from the curvature center are expected for a 1m membrane mirror test article.

Beam focusing

In principle, a single lens can be used for focusing the beams from the Hartmann subapertures. The beams are pencil, and the aberrations are not too critical. Distortion should be assessed beforehand and taken into account as the pencil beams passes the lens at different heights. The diameter of the lens should be no less than the hole array size in order for the dynamic range to be maximum. The F-number of the lens ought to be as large as 1. Otherwise, one will have to use super-large detector to keep the dynamic range wide. We used a lens of 25 mm in dia and 20 mm focal length. Spherical aberrations, coma and astigmatism turn observable

and influence the accuracy of the measurements. Fortunately, the accuracy worsening seems acceptable for the maximum wavefront slopes.

So, the appropriate testing and calibration of the device are required to ensure adequate measurements.

Mirror surface re-imaging

A compact autonomous wavefront sensor should probably analyze a mirror image. It means that a projection lens is needed to re-image the mirror surface into the plane of the Hartmann hole array without any significant aberrations and geometric distortions. Unambiguous correspondence between mirror's zones and corresponding Hartmann subapertures is badly needed. That is why we were trying to eliminate distortion of the lens (the Hartmann hole array is rectangular) and minimize lateral aberrations in order to prevent spreading the energy of the beams over adjacent subapertures. The curvature of the image surface should be also taken into account.

We considered several standard lenses for testing a 20 m membrane mirror of 60 m focal length (see the Phase1 report, Fig.1, page 7). The simplest objective lens to satisfy the above requirements was Triplet of three lenses (f'=100 mm). The distortion was less than 1%, the maximum lateral aberrations were of 0.12 mm.

The diameter of the lens defines the dynamic range of the measurement in the object domain. The expected distortions of the mirror points can be considered enough small (2 mm) to influence the quality of re-imaging. But the rays from the distorted zones possess angular aberrations and do not pass the projection lens in appropriate points. If the projection lens is placed at the focus (curvature center) of the mirror, the maximum measurable angular aberrations is determined by $\Delta\varphi \approx d/2f'$, where d is the diameter of the lens, f' is the focal length of the mirror. In our case

$$\Delta\varphi \approx 3.2 \cdot 10^{-3}\text{rad} \quad \text{(Phase 1 report, page 13),}$$

and the minimum $d = 2\Delta\varphi \cdot f' = 2 \cdot 3.2 \cdot 10^{-3} \cdot 100 = 64$ mm

2.4.Calibration

The calibration is intended for checking whether the device operates correctly and determining amendments needed. The calibration can be conducted by means of simulating known wavefront tilts. We made up a calibration schematic shown in Fig.2.4.

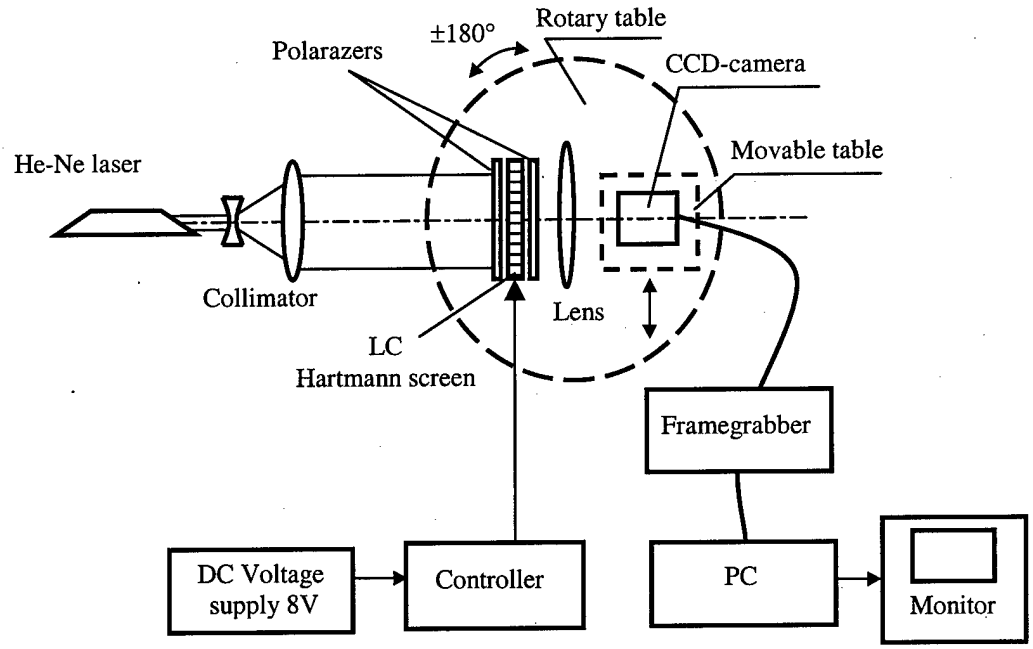

Fig.2.4.

The collimated laser beam illuminates the hole array of the Hartmann sensor under investigation. The Hartmann sensor itself is positioned on the rotary table of a theodolite (range of ±180°, error of less than 1 arcsec). Turning the table simulates wavefront tilts, the same for all Hartmann subapertures. The focusing lens of the sensor forms focal diffraction spots on the CCD-camera where the lateral displacements of spot's centroids are measured. The Hartmann subapertures are turned on consequently with the help of the controller (manually at the first stage of the calibration). Any departures of the measured spot displacements from the calculated ones are supposed to be amendments to measurements and are to be memorized in the computer. We are using Cohu-4915 CCD-camera with the pixel array of 4.8 x 6.5 mm. These sizes are too small to check the sensor operation in a wide dynamic range. The CCD-camera is fixed on the table with micrometric positioning (resolution of 5 μm, range of ±10 mm). When the wavefront tilt is very large (up to 30°) the table is moved in lateral direction until the spot appears on the CCD-array. The spot displacement to be measured equals the table displacement plus the corresponding coordinate on the CCD-array. The displacement of the table along the optical axis allows us to find the optimum position of the CCD-camera and the optimum spot size.

The calibration is in progress at the moment. The expected dynamic range of the LC Hartmann sensor is ±30°. Necessary amendments because of aberrations approach 10 arcmin for large wavefront tilts. The manufactured LC Hartmann sensor and the process of its calibration are shown on photos (see Fig.2.5 and 2.6).

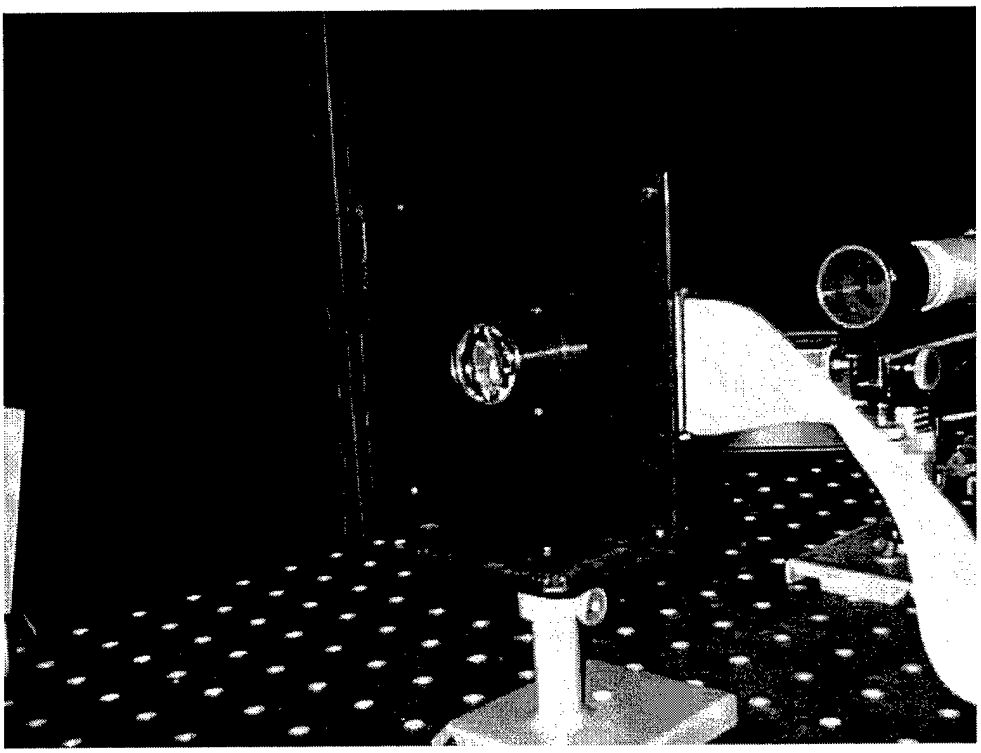

Fig.2.5a

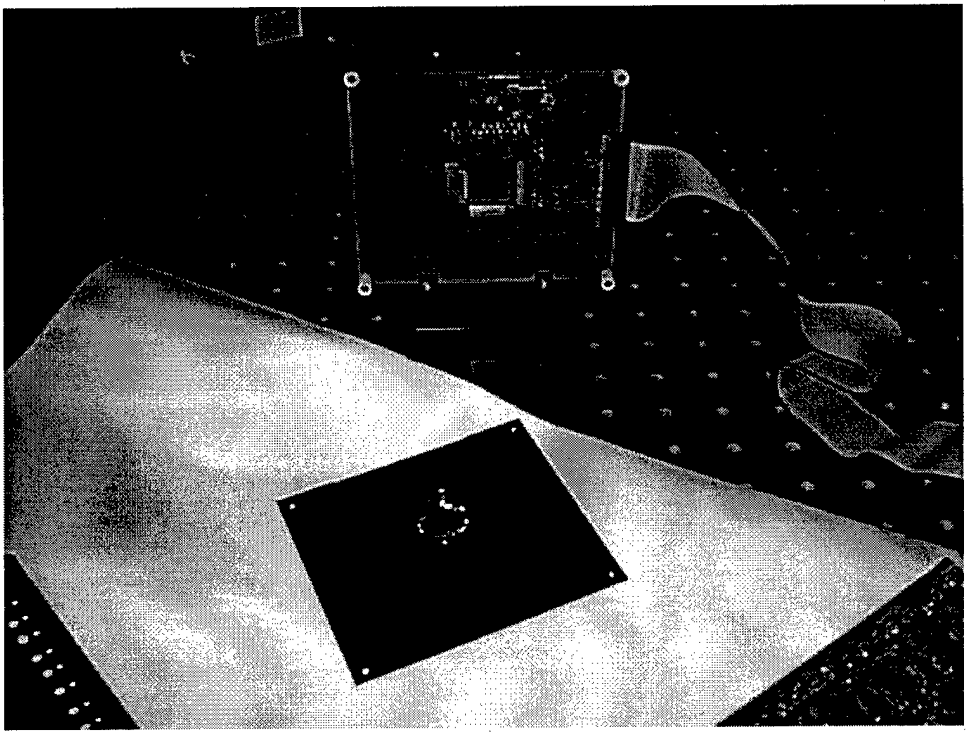

Fig.2.5b

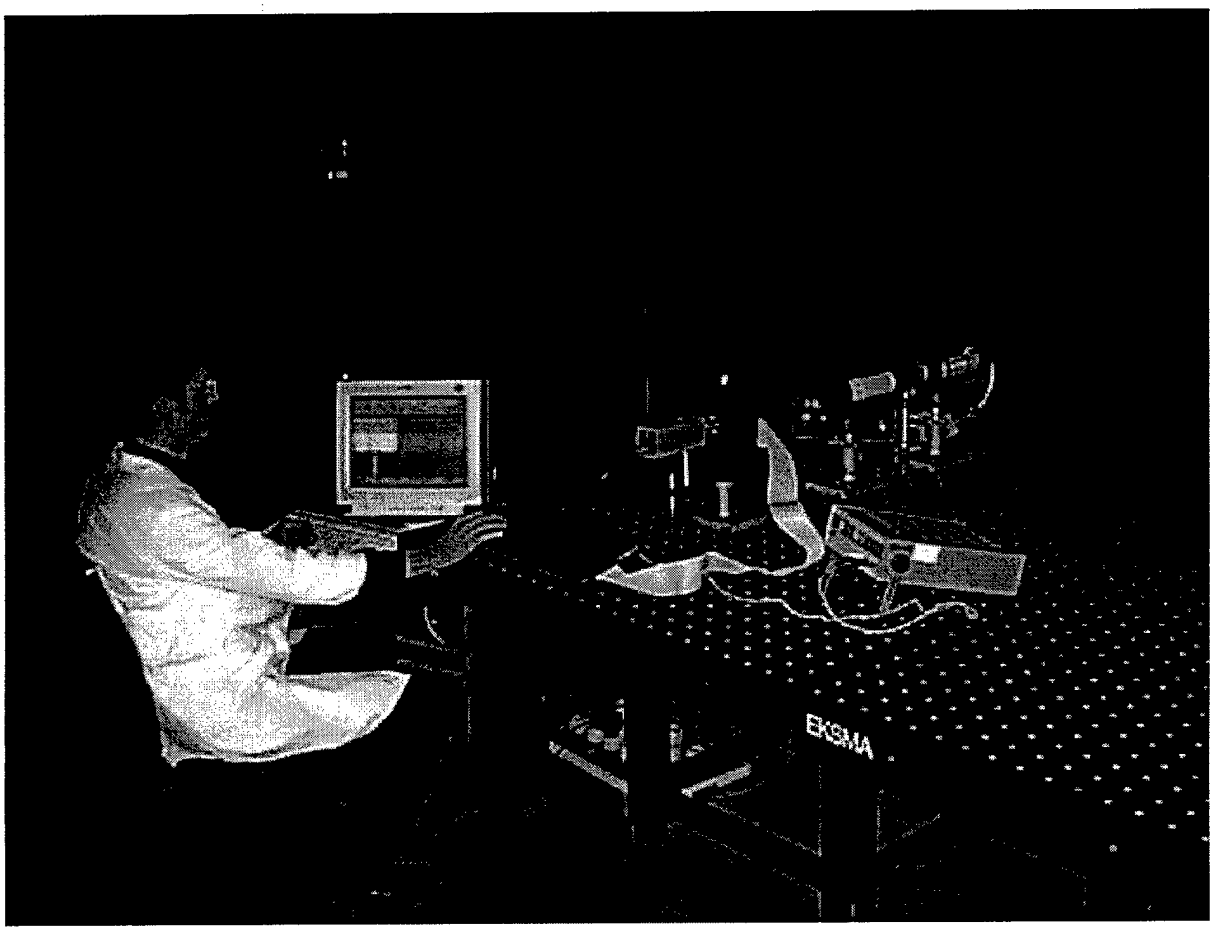

Fig.2.6

3. Two-wavelength dynamic holographic interferometry

3.1. Measuring diffraction efficiency of the optically addressed liquid-crystal spatial light modulators

Earlier, we studied the possibility of using the method of two-wavelength dynamic holography for measurements of severe aberrations of a membrane mirror (see the Phase 2 report). As it was shown, the application of this method allows one to considerably expand a measurement range under certain conditions. Optically addressed spatial light modulators (OASLM) based on the use of the recording liquid-crystal medium, were envisaged to be utilized as dynamic holographic media.

For creation of the effective wavefront sensor (WFS) it is necessary, that OASLM has some unique properties. Firstly, a spatial resolution of OASLM should be as high as possible. To achieve a record measurement range of WFS, the diffraction efficiency of the modulator should be no less than 3...5 % at frequency of 300 mm^{-1} (see the Phase 2 report). Secondly, the spectral selectivity of OASLM should be extremely high. We suppose that it is possible to provide the operation of the two-wavelength holographic converter at a difference of wavelengths of recording and reading beams of 10 nm in the 0.5...0.55 μm range.

The analysis of the available information has shown that, at present, there are no media for recording dynamic holograms to meet the above requirements. That is why, the special investigations and development of the respective technology are required. We plan to implement a series of researches before the beginning of prototyping of the WFS for a membrane mirror. The purpose of these researches is to improve the characteristics of OASLM fabricated at S.I. Vavilov State Optical Institute in order to reach the above mentioned performances.

At the first stage of these investigations, the measurements of diffraction efficiency of OASLM will be made depending on parameters of recording and reading beams (intensity, frequency and duration of the recording pulse, spatial frequency etc.), and also on parameters of applied voltage.

The measurement interferometric setup was assembled (see Fig.3.1). A green CW radiation of a single-frequency, frequency-doubled Nd:YAG laser (λ=0.53 μm), passing through a matched lens, enters the ML-102 commercial electrooptical modulator. The modulator enables to create light recording pulses of any shape and frequencies. Having passed through the

modulator, the laser beam is expanded by the telescopic system, and then it is divided by the splitter plate. Two collimated beams of green light fall on OASLM at different angles. These beams interfere, and a high-contrast interference pattern is formed. The fringe width is approximately equal to $b = \lambda / \sin\alpha$, where α is the angle between beams. The fringe width can be changed within the interval from 2.5 μm (spatial frequency 400 mm^{-1}) up to 50 μm (frequency 20 mm^{-1}) by appropriate linear and angular displacements of mirror 1. The fringe width is measured precisely with the help of the microscope.

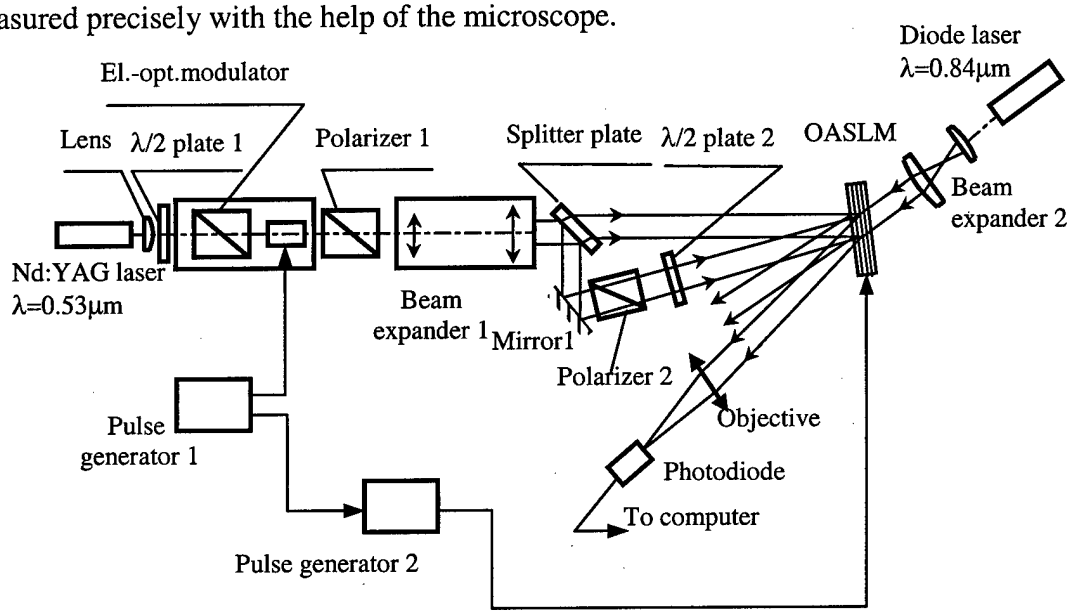

Fig.3.1. Schematic of experimental setup for measuring diffraction efficiency.

Polarizer 2 and half-wave plate 2 are intended for equalization of intensities of the interfering beams, and also for bringing together the polarization planes. The maintenance of these conditions ensures high fringe contrast, approaching 1.

The CW radiation of the diode laser (λ = 0.84 μm) is used as a recording radiation. The intensities of the beams of the first and zero orders are registered with the help of the photodiode. During the registration of the beam of a zero order, half-wave plate 2 is turned in such a manner to make the interference pattern in green light disappear. The diffraction efficiency is determined in experiment as a ratio of the intensities of the beams of the first and zero orders, i.e. not taking into account transmission losses. Photos of the set up assembled are presented in Fig.3.2a, b.

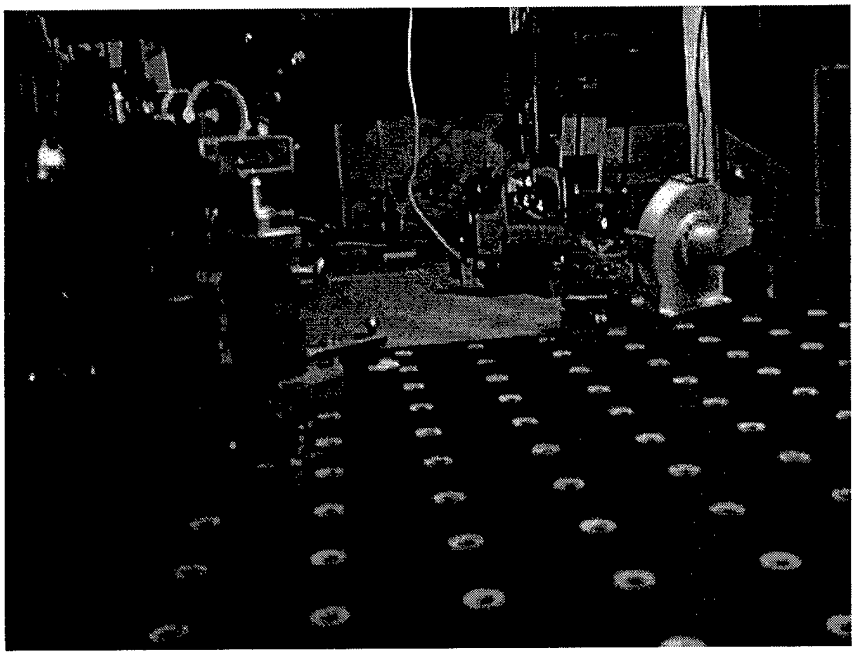

Fig.3.2a

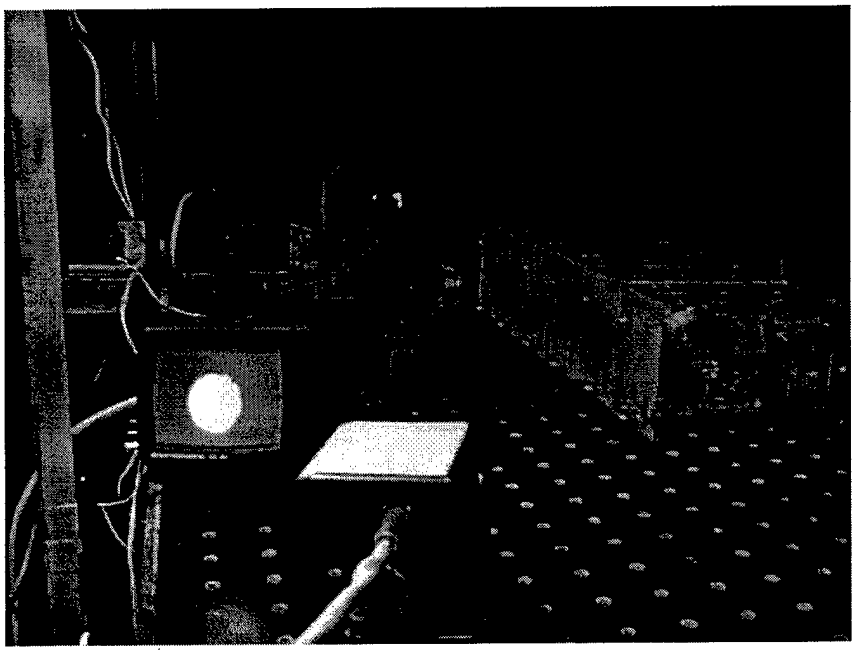

Fig.3.2b

The measurements are carried out in two different operating modes:

- pulse writing light intensity and DC voltage and
- pulse writing light synchronized with pulse voltage of power supply.

It should be noted that frequencies of the pulses of intensities and voltage are low (in the range from 0.1 up to 10 Hz). It is caused by inertia of the liquid-crystal media used. The example of a timing diagram of pulses of writing radiation and voltage is shown in Fig.3.3.

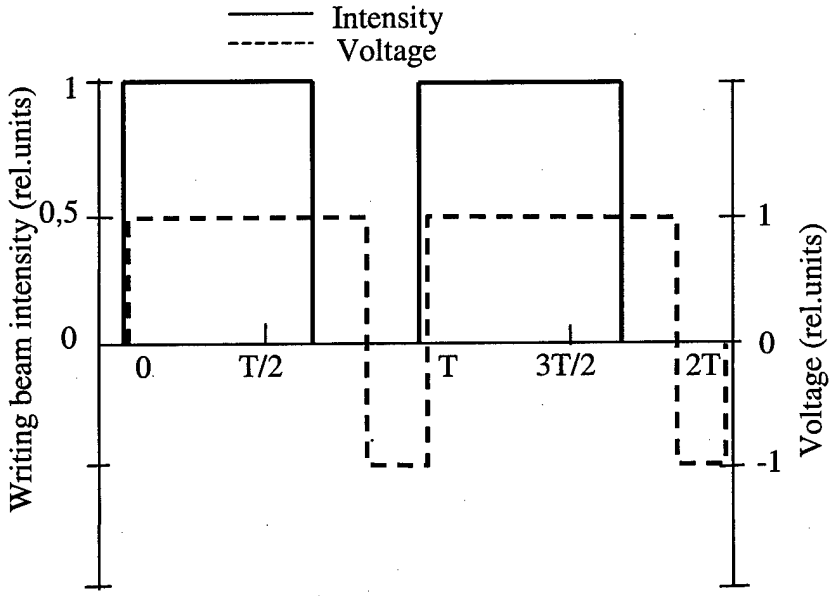

Fig.3.3. Timing diagram for OASLM voltage and writing

We have been investigating OASLM based on the Polyimid Photoconductor – Nematic LC structure (ZKS-1630B, Russian research institute NIOPIK, Moscow) with the following parameters: optical anisotropy $\Delta n = 0.13$, dielectric anisotropy $\Delta\varepsilon = +4.4$, temperature range -20...+90°C. OASLM consists of a number of thin layers sandwiched between two glass substrates: photoconductive layer, transparent ITO electrodes, LC layer, alignment layers and dielectric mirror operating in reflection mode (Fig.3.4). The operating voltage applied to the ITO electrodes is divided between the photoconductor and LC layer proportionally to the writing beam intensity and the conductivity of these layers [2,3]. A photo of OALSM under investigations is presented in Fig.3.5. The expected parameters of OASLM are given in Table 1.

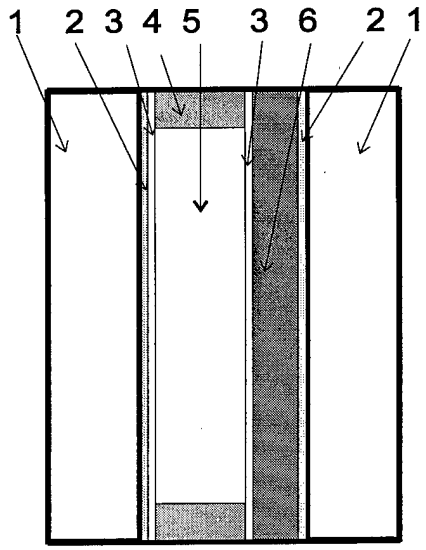

Fig.3.4. Schematic of the transmissive mode SLM based on the photoconductor – liquid crystal structure: 1 - glass substrates, 2 - ITO transparent electrodes, 3 - alignment layers, 4 - spacer, 5 - LC, 6 - photoconductor

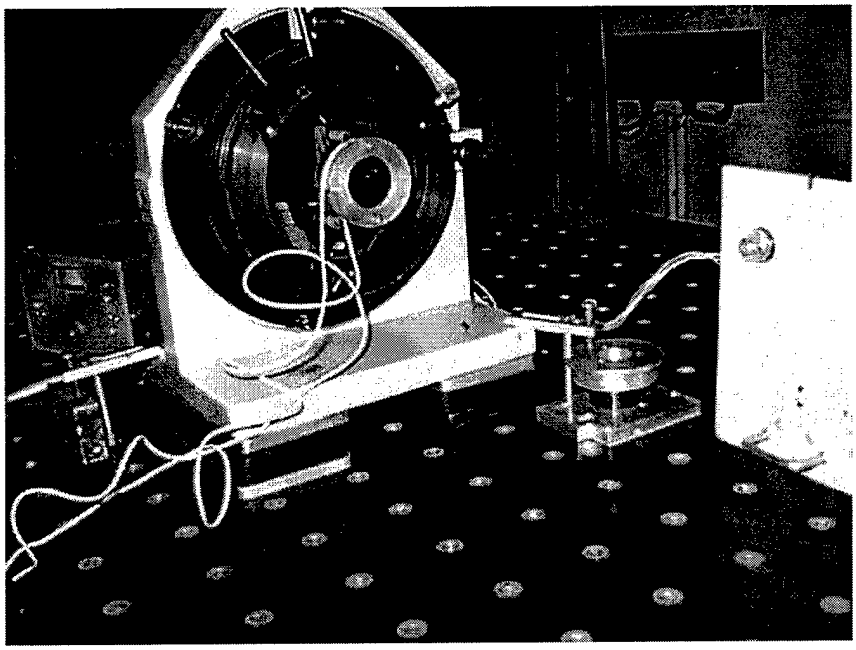

Fig.3.5

Table 1

Specification	SLM based on the PP-NLC structure
Maximum diffraction efficiency (η_{max}), %	30
Spatial resolution at 50% of η_{max} , lp/mm	300
Response speed, Hz	1
Sensitivity ($\eta = \eta_{max}$), $\mu W/cm^2$,	1000
Writing wavelength, nm	400...630
Reading wavelength, nm	600...1100
Aperture, cm^2	6
Used electro-optical effect	S-effect

3.2. Practical suggestions

The WFS with two-wavelength liquid-crystal holographic converter can be implemented in accordance with the diagram shown in Fig.3.6. A severely deformed spherical mirror is used as an object under test. The diode-pumped frequency-doubled Nd: YLF (λ_1= 526.5 nm) and Nd: KGW (λ_2=533.6 nm) lasers are used as laser sources. Two collimated beams at λ_1 and λ_2 illuminate the achromatic lens which forms two spatially coincided spherical waves, diverging from the curvature center of the mirror under test. The coincidence of the beams is provided with the dichroic beam splitter. It is transparent for the beam at λ_1 and reflective for the beam at λ_2. Aberrated beams reflected from the tested mirror are collimated and directed to OASLM. The beam at λ_1 is used for recording the dynamic hologram. The plane wave at λ_1 is the reference one. The second aberrated beam is used for reconstruction of the converted aberrated beam.

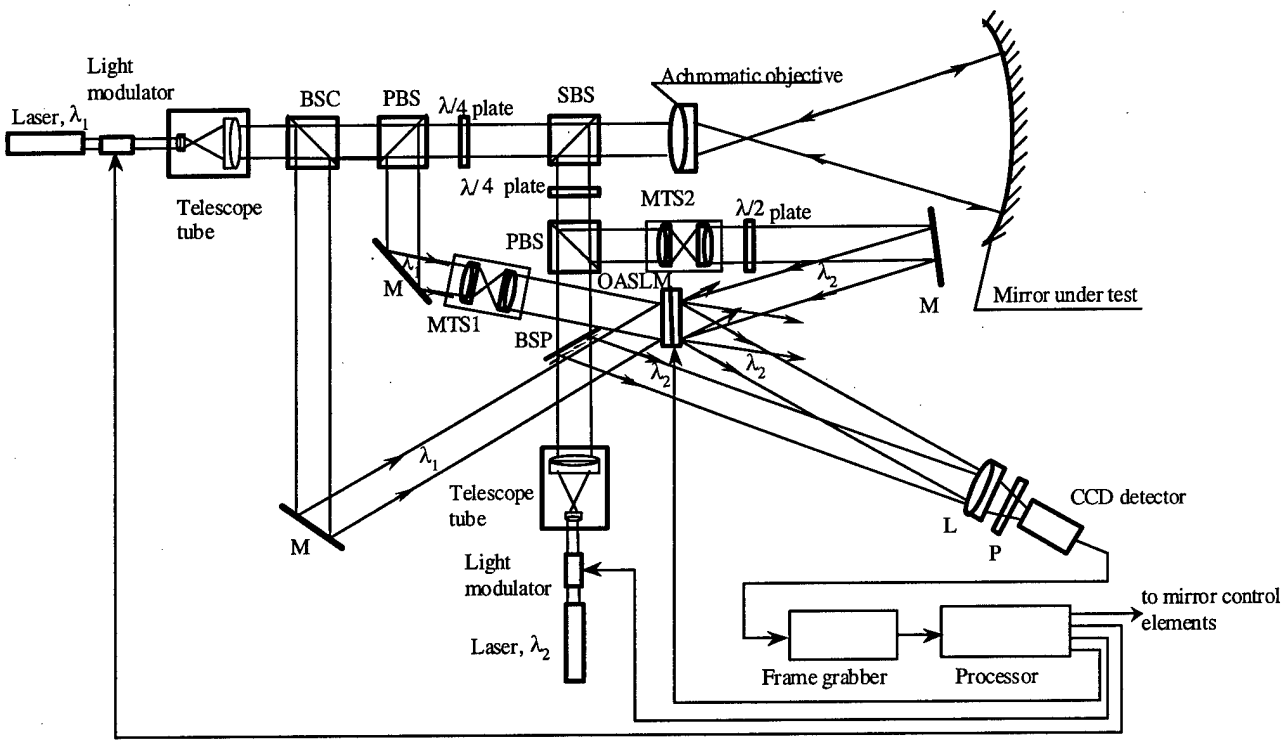

Fig.3.6. Diagram of the WFS with two- wavelength dynamic holographic converter.

OASLM - optically addressed liquid-crystal spatial light modulator; PBS - polarization beam splitter; BSC - beam splitter cube; SBS - spectral beam splitter; M - plane mirror; BSP - beam splitting plate; L - lens; P - polaroid, MTS1,MTS2- matching telescope system.

To ensure high spectral selectivity of hologram recording, OASLM is illuminated by light pulses at λ_1 and λ_2. The pulse voltage is also applied to OASLM. Electrically addressed liquid-crystal light modulators are used for light modulation. The synchronized voltage pulses applied to the modulators and the OASLM are generared in the processor. OASLM contains a dielectric mirror between photoconductor and liquid crystal layer. Such a structure is convenient because it allows one to direct the reading beam at λ_2 from the opposite side (liquid crystal side).

The beams reflected from the mirror under test pass other paths in reverse direction due to the quarter-wave plates. The axes of the plates are at the angle 45^0 to the ones of polarizing beam splitters (PBS). After double passage of the polarized beam through the plates, its polarization directions are turned at 90^0. The reconstructed wave at λ_2 with decreased phase distortions ($\lambda_1/(\lambda_1-\lambda_2)$ times) interferes with the reference wave at λ_2. Lens L images the mirror under test along with interference pattern on the photodetector array. All elements of the WFS, excepting the videocamera and processor, are fabricated at S.I.Vavilov State Optical Institute.

The suggested WFS can easily change the mode of its operation: from coarse measurements immediately after deployment of the mirror to the mode of mirror surface maintenance. In the first mode, the WFS generates the control signal for the controllable membrane mirror. In the second mode, the WFS forms the control signals for a small deformable wavefront corrector. An accessible exit pupil of the telescope where the small corrector is to be placed should be formed in this case.

For the first mode of measurements, we hope to provide operation at a maximal fringe density on the OASLM of 200 fringes/mm or at a gradient of path difference changes of 100μm/mm. For a membrane mirror of 10-m diameter, it corresponds to local, steep slopes of the membrane mirror surface up to 0.3 mrad .

The transition to the second operational mode is provided by changes of the reading wave and the photodetector system. The reading wave should become a plane wave at λ_1, which was used for dynamic hologram recording at the first measurement stage. The measurement range is decreased but the accuracy increases. This accuracy is sufficiently high to provide the possibility of obtaining diffraction quality of the image.

4. Preliminary comparison of LC Hartmann sensor and two-wavelength dynamic interferometry

As was shown, both LC Hartmann sensor and two-wavelength dynamic interferometer are potentially capable of measuring severe aberrations. No obvious advantages of either of the methods were found. They have "pluses" and "minuses". Additional investigations are needed, in particularly, experimental ones. Nevertheless, some preliminary comparative estimates would be very helpful. Table 2 gives such information. The most important criteria are used for comparison.

Table 2

Criterion	**LC Hartmann sensor**	**Two-wavelength dynamic interferometry**
Dynamic range	Angular aberrations up ±30° +	Wave aberrations up to thousands waves +
Sensitivity	-	+
Simplicity and reliability	+	-
Possibility of real-time mode of operation	Scanning mode -	+
Perspectives of miniaturization	+	+

"+" means that the method absolutely meets the requirement,
"-" there are some doubts .

Miniaturization is expected on the basis of available or actively developing technologies. The methods measure different aberrations – angular and wave. This adds some complexity to the comparison. The dynamic range of the holography is defined by spatial resolution of the medium . We can use the resolution to calculate the wave and angular aberration for the same object, for example, a membrane mirror.

The comparison will be complete after extensive experiments, including metrological estimates.

5. Membrane mirror for further investigations

Either some object for measurements or physical simulation of different wavefront deformations are required for experimental investigations. We manufactured and are exploring a membrane mirror of 212 mm clear aperture. In our opinion, it allows as to approach a realistic situation, at least at the stage of large mirror prototyping . A drawing of the mirror is given in Fig.5.1.

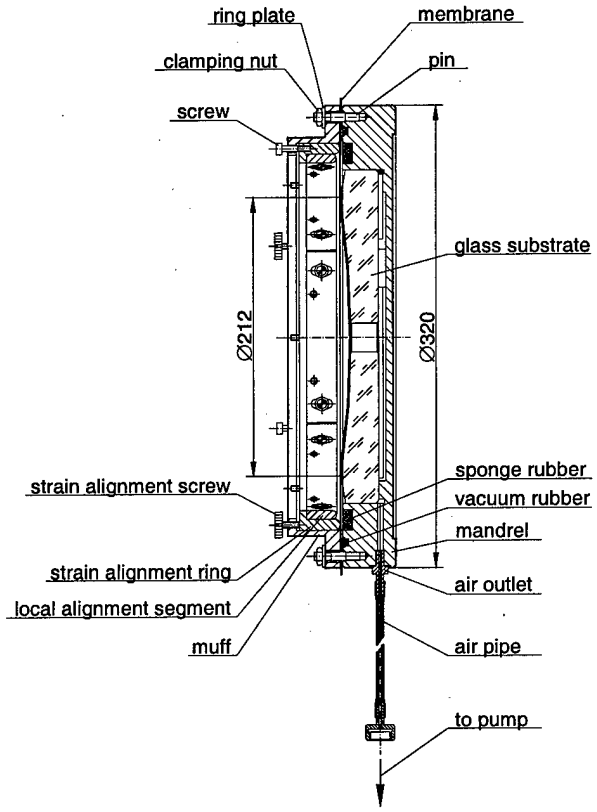

Fig.5.1.

The membrane is stretched over the rim annulus of the glass substrate. The annulus is of optical quality (0.1 λ RMS, λ=0.63 μm). The substrate is made from a lens by means of partial removing the central part of the lens (by grinding and polishing) and drilling the central hole to vacuum the inner space of the substrate. The substrate is fixed in the mandrel that has the air outlet for vacuuming. The mandrel itself is clamped to the muff with pins and nuts through the membrane. There is the ping of vacuum rubber near the rim of the mandrel to ensure the hermeticity of the clamping and keep the inner chamber vacuumed. The strain alignment metallic ring with well polished surface is fixed to the muff. The strain alignment is conducted with the adjusting

screws. The ring of six segments for local strain alignment is also available. The photo of the mirror is presented in Fig.5.2.

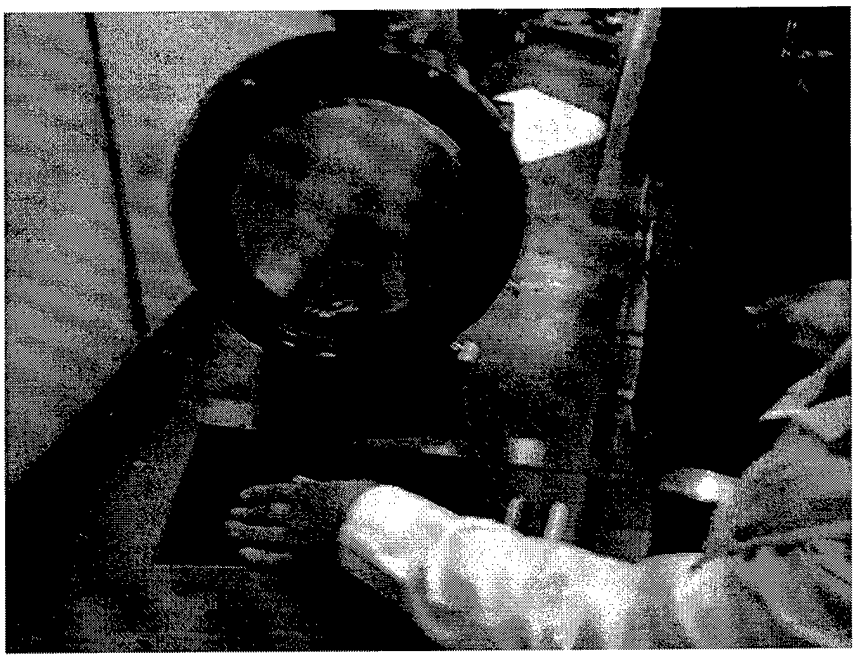

Fig.5.2.

The Lavsan polymer film with aluminium coating (made in Russia) is used as a membrane. It was hot intended for optical applications. Interferograms of the plane mirror are shown in Fig.5.3 and 5.4 that illustrate the quality of the film after the strain is applied. Fig.5.3a, b are the IR interferogram and reconstructed topography of the mirror at λ=10.6 μm, Fig.5.4 is the interferogram of the plane at λ =0.63 μm. The RMS wavefront deformation is about 1.2 μm (0.1λ at 10.6 μm). The ripple structure remains even under the maximum strain . The film can be probably used in IR range.

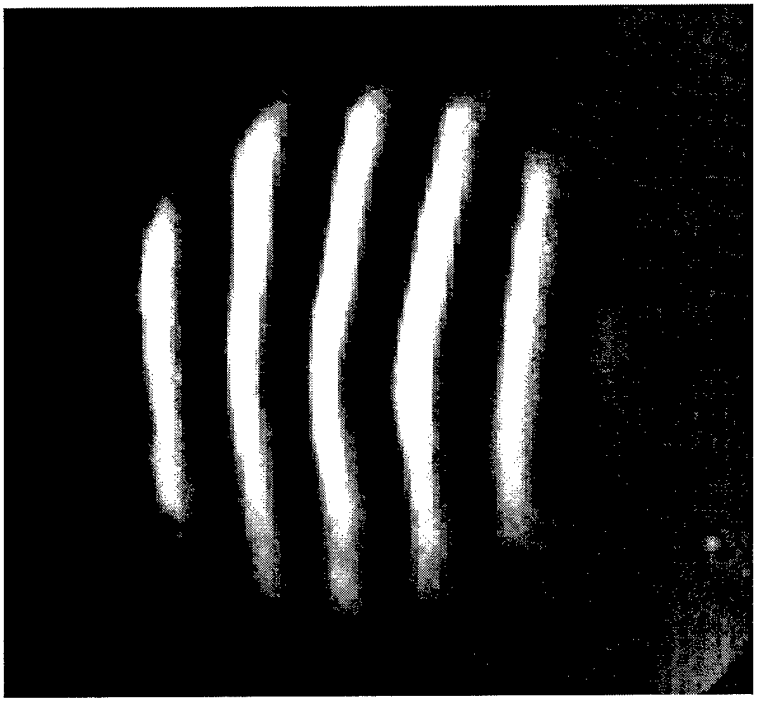

Fig.5.3a

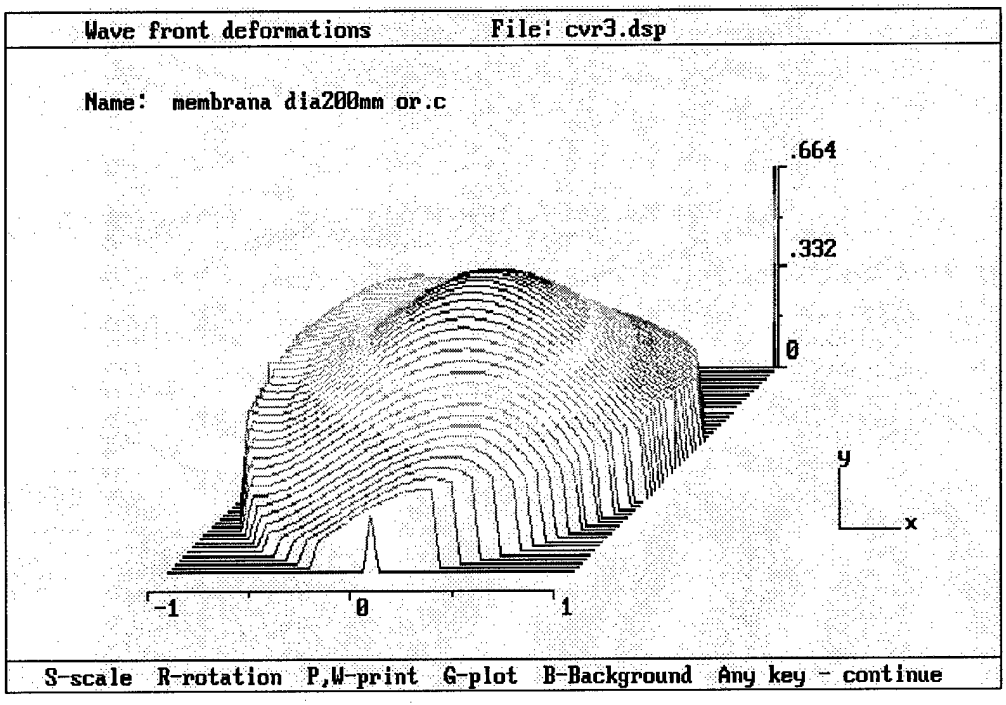

Fig.5.3b

After vacuuming, the membrane mirror becomes aspherics of higher order. Fig.5.5 is the interferogram of the mirror of 700 mm curvature radius (f–number 1.65) at λ=10.6 μm. Practically all the surface is seen. The large disk corresponds to the sensitive surface of pyrocamera.

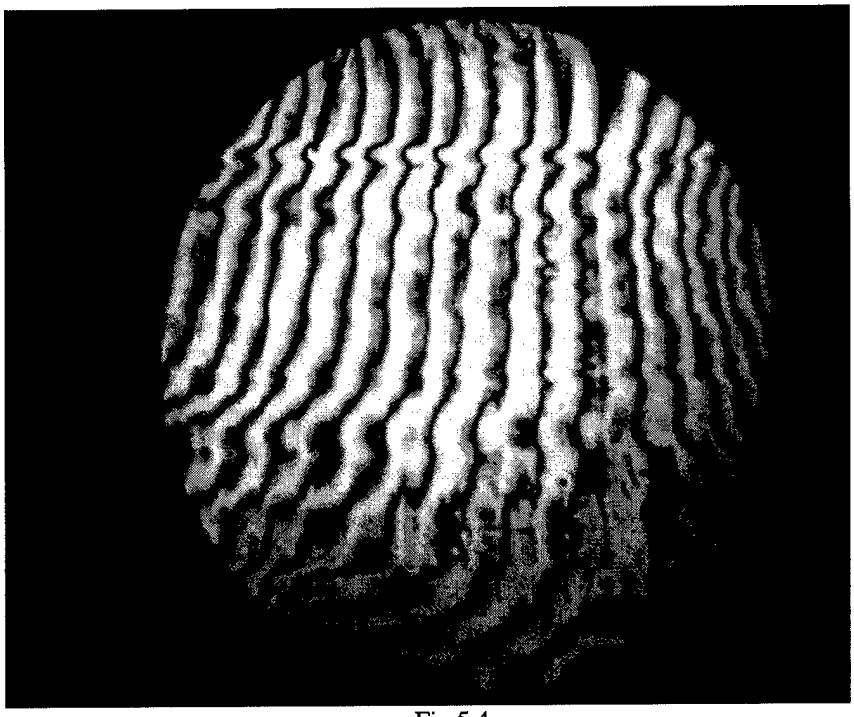

Fig.5.4

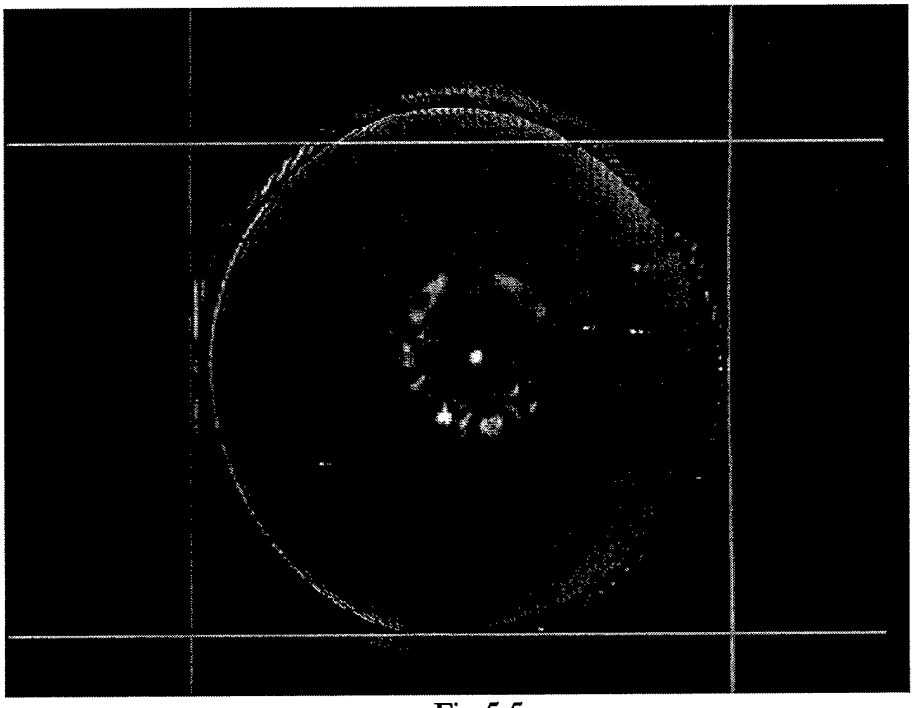

Fig.5.5

6. Summary table of considered methods

Finishing the current study, we can make up a summary table of the methods considered. Table 3 includes the brief information on pros and cons for every method as well as special comments and recommendations.

Table 3

Method	Pros	Cons	Notice
Focal spot	1. simplicity, 2. no hologram needed	only coarse test	preliminary alignment
Collimation	unlimited dynamic range	1. only local tilts, 2. alignment needed	Auxiliary
LC-based Hartmann-Shack	1. large dynamic range, 2. tunable sensitivity	Real-time operation impossible (scanning)	Under investigation
Acousto-optic Hartmann	1. dynamic range up to 10 deg. 2. High resolution	1. scanning, 2. low diffraction efficiency	Promising, acousto-optic holography is perspective
Curvature sensing	simplicity (only intensity measurements)	1. complexity of error reconstruction, 2. limited range because of beam crossing	Under investigations, widely used in observatories
Intensity relationships	simplicity (only intensity measurements)	1. accuracy limited, 2. uniform illumination needed	theoretical
Shearing interferometry	1. large dynamic range, 2. low coherency light source, 3. tunable sensitivity	Complicated error reconstruction	Scene-based version attractive
IR-interferometry	Large dynamic range	Cooled lasers and detectors	Technologically not analyzed
Two-wavelength interferometry	1. large dynamic range, 2. tunable sensitivity	Complexity of schematic	Under investigation (especially in IR)
Two-wavelength dynamic holography	1. large dynamic range, 2.tunable sensitivity, 3. image correction possible	Special complexity of schematic	Under investigations
Scene-based sensing	1. no hologram needed, 2. large dynamic range	Scene needed	Lateral shear, very promising
Method of coincidence of the interference orders fractional parts	1. large dynamic range, 2. tunable sensitivity (covers all regimes)	1. many light sources, 2. huge error possible	perspective

White light interferometry	1. large dynamic range, 2. no coherent source needed	1. scanning, 2. movement along axis may be needed	For alignment in shop (laboratory)
Laser profilometry	large dynamic range	scanning	technological
Moire	1. simplicity, 2. no hologram needed	Diffuse structure for operating light needed	To be investigated

(Table 3, continued)

Scanning white light interferometer is a conventional equal path one. A reference beam in it reflects from a reference moving mirror. The movement of the mirror results in displacement of achromatic fringe on the surface under test. The amount of the reference mirror shift from the initial position is equal to the departure of the surface zones where the achromatic fringe is located.

It is seen from the table that all the methods have advantages and drawbacks. The most promising methods are Hartmann sensing, two-wavelength holography and IR interferometry, shearing scene-based sensing. We believe these methods are worth separate investigating from the point of view of their modernization. The corresponding devices can be utilized not only for measuring large membrane mirrors but also in optical shops for testing deep aspheric optical surfaces of higher order (very actual task at the moment).

7. Summary and conclusions

Two concepts of building a compact autonomous measuring system for large membrane mirror (10...20 m in diameter) have been developed in the scope of the study. According to the statement of task, the measuring system must operate in the dynamic range of 1 to 2000 μm with the changeable accuracy within the range of 0.3...100 μm. The wavefront slopes are supposed to reach 3...5 mrad. The complexity of the task is confirmed by the fact that all known measuring systems have 10...15 times lower parameters. This determined the character of the study.

We have comprehensively considered 14 methods (interferometric and noninterferometric) from the point of view of their maximum dynamic range. Our comparative theoretical analysis and preliminary experiments with available facility allowed us to select three methods for deeper analysis and experimental investigations:

- Hartmann method;
- Two-wavelength holographic interferometry;
- curvature sensing (by Roddier).

Conventional Hartmann-Shack wavefront sensors usually fail to measure huge angular aberrations (wavefront tilts) because of the problem of "beam crossing" after the Shack lenslet array. The problem is partially solved if a moving lens consequently images the lenslets and their focal spot on the detector to track the beams. We have chosen another approach concerned with the realization and operation of the Hartmann hole array (or Shack lenslet array). It can operate as a scanner, with subapertures to be turned on one by one in desired order. Such arrays can be implemented on the basis of liquid-crystal spatial light modulators, components with phase changes, acousto-optic cells, multi-element controllable MEMS-mirrors, etc.

A concept of LC Hartmann wavefront sensor has been developed. Three versions are suggested:

- LC Hartmann-Shack sensor with controllable LC lenslet array;
- Hartmann-Shack sensor with conventional Shack lenslet array and LC lens with tunable focal length behind the array;
- LC sensor with Hartmann hole array and focusing lens.

The third (simplest) version has been used in creating a LC Hartmann sensor which is under calibration at the moment.

Also, a concept and a principal and functional optical configuration of a wavefront sensor on the basis of two-wavelength holographic interferometry have been proposed. The main difference between our ideas and the approach by V.Venediktov, M.Gruneisen et al [4] is that our group has found some ways to substantially increase the equivalent wavelength (up to 30...40 μm) due to diminishing the difference between the wavelengths of recording and reconstructing radiations. That allows us to increase the dynamic range of measurements. The set up for measuring diffraction efficiency of dynamic holograms were made up.

Two concepts of the wavefront sensor have been preliminary compared according to the most important criteria: dynamic range, sensitivity, simplicity and reliability. Much deeper comparison is needed on the basis of experiments. To approach the reality as close as possible we have manufactured a membrane mirror of 212 mm in diameter as an object for investigations.

The dynamic range of the curvature sensing method has been found rather limited. We have not managed to reconstruct the profile of severely deformed mirror with acceptable accuracy. Additional computer and physical experiments are highly needed.

On request of the customer, we considered the possibilities to measure the deformations of large mirrors (10...20m) during the study. From the very beginning, the consideration showed that a problem of too large focal spot existed. It means that the whole surface of the mirror cannot be observed immediately after deployment with a lens of acceptable sizes regardless of what method of measurements is used. A very large projection lens is needed to collect all the beams reflected from the mirror. But the requirement of compactness is violated in this case. One of the possible solutions of the problem is to measure deformation in two stages: simple focal spot method (not very sensitive) followed by Hartmann or interferometric measurements.

Finally, we should note that a general nature of the task made us to search for new ideas in different directions simultaneously. This did not allow our group to complete all desired experiments under conditions of financial and time constraints. Unfortunately, a comprehensive experiments on shearing interoferometric scene-based wavefront sensing and IR two-wavelength interferometry were outside our study. Nevertheless, these methods remain very attractive, and we believe it would be reasonable to continue investigations in these areas in the scope of a new study.

Besides the profound analysis of different methods and modernization of available components, we paid attention to the questions of system engineering. In particular, possibilities of creating miniature measuring smart-systems are of great interest to us. Such systems could be

implemented on the basis of the latest technological establishments in integrated optics, micro- and nano-structures, modern ultra-light-weight material and computers.

Another possible direction of investigations can be concerned with the telescope system as a whole. Some ideas arose when we worked at the membrane mirror prototype. Our many year experience in ultra-light space-based optical telescopes (including deployable segmented mirrors) convinces us that the best diagnostic subsystem can be developed only by considering the telescope as a complicated system. Only such an approach can help us to find the optimum ways of building the diagnostic and control subsystems. In connection with the above said, we believe a complex (system engineering) work at the problems of folding (packing), transporting to space and deploying a membrane mirror, including diagnosing itself, would be very helpful for the customer as a separate direction of our further works.

8. References

1. V.Laude, S.Olivier, C.Dirson, J.-P.Huignard// Hartmann wave-front scanner/Optics letters, 1999, Vol.24, № 24, pp.1-3.
2. N.Collings, A.R.Pourzand, F.L.Vladimirov, N.I.Pletneva, A.N.Chaika// Optical Memory and Neural Networks, No 6, 1997, pp.187 – 198.
3. F.L.Vladimirov, A.N.Chaika, N.Collings// Spatial Light Modulator based on the hydrogenated amorphous silicon/deformed-helix ferroelectric liquid crystal structure: influence of dielectric mirror. The 7-th International conference on Ferroelectric Liquid Crystals, Darmstadt University of Technology, Germany, 1999, pp.162-163
4. V.Yu.Venediktov, V.A.Berenberg, A.A.Leshchev, M.V.Vasil'ev, M.Gruneisen // Two-wavelength dynamic holography. Proc.of SPIE, 1999, Vol.3760, paper N27.